

## Control's Fundamental Coursework

### Summary

This report covers the modelling and control design of the Quanser Aero2 Dual-Rotor system, configured in a 1 degree-of-freedom setup. MATLAB, SIMULINK, and QUARC software were used to develop the models. The system consists of two subsystems: the rotor and pitch subsystems. A cascade control structure was applied, with the inner loop controlling rotor speed and the outer loop regulating pitch angle. Step responses were used to identify the systems model parameters. These models were validated against the physical system. Controllers were designed to achieve the desired system, and simulation results were compared with physical measurements to assess control performance.

### Introduction

The experiments done in the lab session aims to achieve the modelling and control of the Quanser Aero2 Dual-Rotor system. It is a nonlinear system that is equipped with two DC motors that are functionalized to regulate the pitch angle ( $\theta$ ) through rotor thrust. The Aero2 system is configured in a 1 degree-of-freedom setup where only the pitch angle is only to be controlled while the yaw angle is kept at fixed position. It is consisted of two subsystems: the rotor subsystem (inner loop), which manages rotor speed ( $\omega$ ), and the pitch subsystem, which adjusts the pitch angle by setting targets for rotor speed. The rotor subsystem is modeled as first order system, while the pitch subsystem is represented as a second-order system model. The control structure of this system is illustrated in a block diagram shown by Figure 1. As illustrated in the block diagram, the control structure used is a cascade control, where the inner loop is controlled by a proportional-integral (PI) controller for rotor speed regulation, while the outer loop employs a proportional-integral-derivative (PID) controller to maintain the desired pitch angle. Experiment parameters, such as steady-state gain ( $K$ ), time constant ( $\tau$ ), natural frequency ( $\omega_n$ ), and damping ratio ( $\zeta$ ) were identified to develop system models for control design.

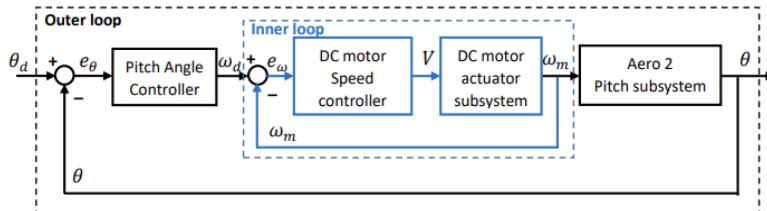


Figure 1 Cascade control structure for 1 DOF Aero2 system

### Results and Discussion

In task 1, the transfer function of the rotor subsystem was estimated by analyzing the system's step response for an input of 10 V. This estimation involved calculating the steady-state gain ( $K$ ) and the time constant ( $\tau$ ), both of which were determined from the step response plot shown in Figure A in the Appendix. From Figure A, the steady-state gain was calculated as ratio of the change in output response ( $\Delta y$ ) to the change in input ( $\Delta u$ ), yielding a value of 18.704. This differs from the value shown in Figure 2.2 of the module, which is 20. The system's time constant, defined as the time required for the system to reach 63.2% of its final value, was determined from Figure A as 1.16 s. With these values of  $K$  and  $\tau$ , the estimated transfer function of rotor model is obtained as follows:

$$G(s) = \frac{18.704}{1.16s + 1} \quad (1)$$

In task 2, the estimated values for  $K$  and  $\tau$  were entered into the SIMULINK model for model validation. The simulated response was then compared with the response of the physical Aero2 rotor model. Figure 2 visualizes the comparison between the physical speed response against the simulated response. As shown in Figure 2 below, there is a noticeable discrepancy between the two responses, with the most significant difference being that the physical response is much faster than the simulated response. The physical response reaches steady state more quickly and with a sharper rise compared to the simulated response. Ideally, the time constant should be smaller than the obtained 1.16 s. In a first-order system, the response is expected to follow a simple exponential rise toward the steady-state value. However, this pattern is not observed in the physical response, implying that it may not be a truly first-order system. This difference could indicate the presence of higher-order dynamics or nonlinear elements. Also, while there is the possibility of measurement errors contributing to this discrepancy, the consistent pattern obtained in the physical response suggest that this is less likely.

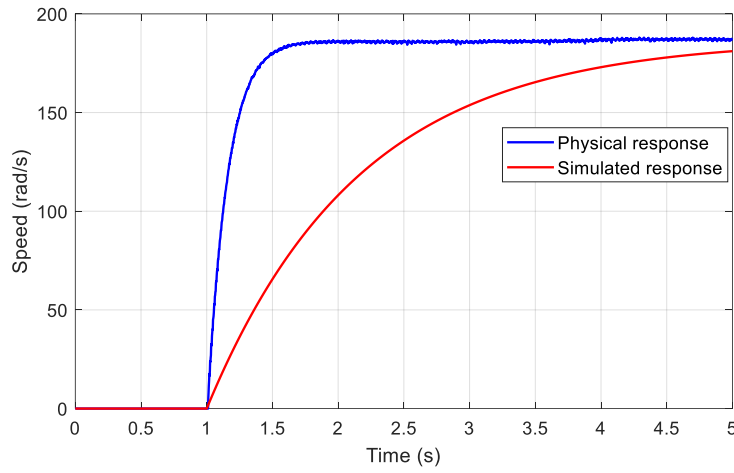


Figure 2 Comparison of responses in rotor subsystem

In task 3, systems parameters for the pitch subsystem, such as the viscous damping ( $D_{vp}$ ), stiffness constant ( $K_{sp}$ ), and the force gain relative to the rotor speed ( $K_{pp}$ ) are determined from measured values including the natural frequency ( $\omega_n$ ), damping ratio ( $\zeta$ ), decrement ratio ( $\delta$ ), period of oscillation ( $T$ ), steady state pitch value ( $\theta_{ss}$ ), and input speed ( $\omega_{in}$ ). These measured parameters are obtained by observing the pitch and speed response to a step input of 7 V, which is turned off after 60 s to allow the system to oscillate freely. The pitch and speed response are shown in Figure B in the Appendix. Since the number of free oscillations is 7, the voltage factor is not increased. Using the values highlighted in Figure B, the measured parameters are as follows:  $T = 8.55$  s,  $\omega_{in} = 134.8$  rad/s,  $\theta_{ss} = 0.418$  rad, and  $\delta = 0.105$ . Accordingly, the natural frequency and damping ratio are calculated as,  $\omega_n = 0.735$  rad/s and  $\zeta = 0.0167$ .

In task 4, using the values of  $\omega_n$ ,  $\zeta$ ,  $\theta_{ss}$ , and  $\omega_{in}$ , the parameters  $D_{vp}$ ,  $K_{sp}$ , and  $K_{pp}$  were computed and loaded into the SIMULINK model for validation. The simulated response was then compared with the response of the physical Aero2 pitch model, as visualized in Figure 3. The simulated model assumes that the pitch subsystem acts as a second-order system, where the main parameters such as the stiffness constant ( $K_{sp}$ ) influence the oscillation frequency, and the viscous damping parameter ( $D_{vp}$ ) affects the rate of decay. As shown in Figure 3, there are noticeable differences between the physical and simulated response, especially in the initial part of the response. In this part, a phase shift is observed, with the simulated response leading the physical response. This phase shift could result from the model's simplified assumption of constant damping and stiffness, whereas in real-world physical systems, these parameters

may be nonlinear and vary slightly with changes in pitch angle and rotor speed. Additionally, unmodeled parameters such as friction could cause delays or shifts. During the free oscillation phase, the phase alignment between the responses improves, suggesting that the model's natural frequency is close to that of the physical system. However, the simulated response shows a higher frequency of oscillation and larger amplitudes than the physical response, which may imply that  $D_{vp}$  is underestimated, resulting in insufficient damping.

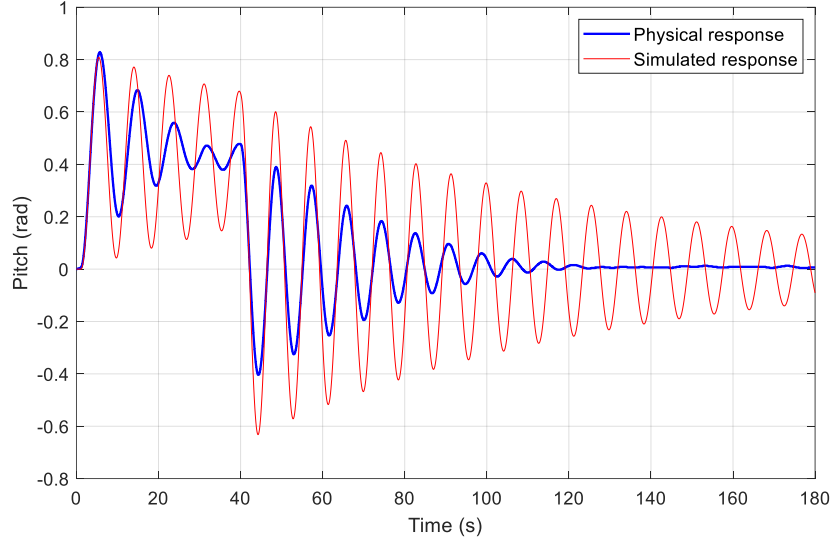


Figure 3 Comparison of responses in pitch subsystem

In task 5, control design for the rotor subsystem (inner loop) involves familiarizing with the proportional controller by testing different gain values to understand their effects on system response. After experimentation, a proportional gain of  $k_p = 0.4$  is set, and the response of the physical Aero2 system is observed. The speed response of the physical system, given a desired speed of 100 rad/s, is shown in Figure C in the Appendix. Due to noise in the output response, the average steady-state value is calculated manually in MATLAB to be 89.07 rad/s, resulting in a steady-state error of 10.93% between the desired and measured speeds.

In task 6, the proportional gain  $k_p = 0.027$  and integral gain  $k_i = 0.099$  were hand calculated by matching the second-order closed-loop characteristic equation to the given specifications of 15% overshoot and a peak time of  $2.5\tau$ . These PI gain values produced the desired produce the desired response in simulation, as shown and highlighted in Figure 4, with overshoot and the target peak time achieved. However, when applied to the physical Aero2 system, the measured response differed. It had a faster initial rise, with a smaller time constant (1.48 s) than that of the simulated response (2.07 s). Also, no overshoot is observed and had a gradual approach to steady state, as shown in the measured speed plot of Figure 4. The discrepancy between the simulated and measured responses could be due to dynamics in the system that the model does not include. These system dynamics may involve unmodeled damping effects, such as friction and air resistance, which increases the damping ratio and reduce overshoot.

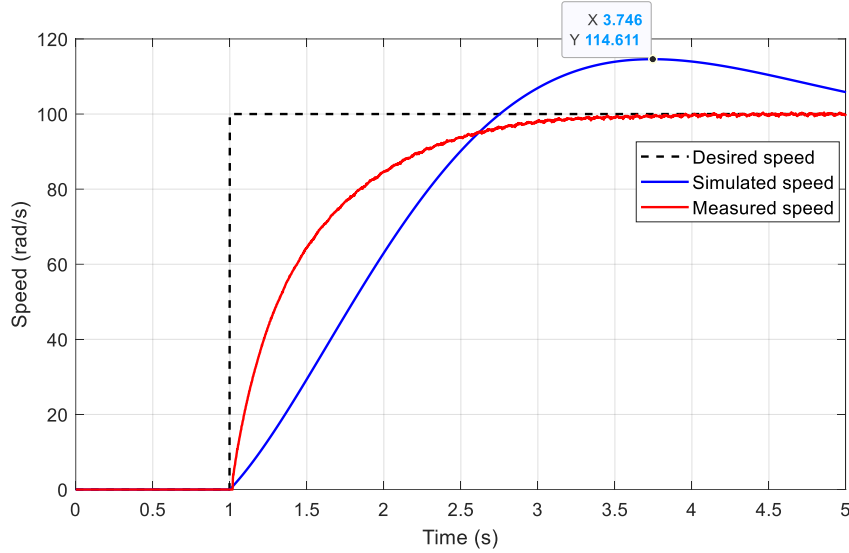


Figure 4 Comparison of responses in PI controlled inner loop

In task 7, the proportional integral derivative (PID) controller was implemented for the pitch subsystem (outer loop). The values of  $k_p$ ,  $k_i$ , and  $k_d$  are tuned iteratively to achieve the desired specifications of small overshoot and low oscillations. Starting with the controller gain values used from task 6, the gains were gradually increased up to 20 times its original value, resulting in final values of  $k_p = 5.5$ ,  $k_i = 20$ , and  $k_d = 40$ . These values were then loaded into SIMULINK for simulation, yielding the measured pitch for a demanded pitch of 0.35 rad, as shown in Figure D in the Appendix. The results showed no overshoot is and only minor oscillations, making the configuration suitable for validation with the physical Aero2 system. These values of  $k_p$ ,  $k_i$ , and  $k_d$  were then applied to the physical Aero2 system, resulting in the response shown in Figure E in the Appendix. In Figure E, the initial response displayed oscillations, which then gradually settled near the demanded pitch of 0.3 rad. The relatively high  $k_i$  value suggests that the controller is strongly focused on reducing steady-state error. However, this high  $k_i$  may also contribute to sustained oscillations. The value of  $k_d$  might still be too low to fully balance the effect of  $k_i$ , thus not being able to provide enough damping effect. Additionally, the  $k_p$  value may be to low relative to  $k_i$ , resulting in a slower initial response.

In task 8, the transfer function from the input voltage to the motor speed is derived into the following transfer function:

$$\frac{\Omega_m(s)}{V_m(s)} = \frac{k_t}{R_m J_{eq} s + R_m k_{dd} + L_m J_{eq} s^2 + L_m k_{dd} s + k_m k_t}$$

In task 9, the derived closed loop transfer function is from the transfer function of task 2, shown in Equation (1), is:

$$\frac{E(s)}{R(s)} = \frac{1.16s + 1}{1.16s + 1 + 18.704k_p}$$

By using final value theorem, SSE to  $\omega_0 = 100$  rad/s is:

$$\begin{aligned} SSE &= \lim_{s \rightarrow 0} s \cdot E(s) \\ &= \lim_{s \rightarrow 0} s \cdot \frac{1.16s + 1}{1.16s + 1 + 18.704 \cdot (0.4)} \cdot \frac{100}{s} = 11.79\% \end{aligned}$$

The computed value of SSE is larger than the obtained SSE value of task 5 which is 10.93%

In task 10, the transfer function from the rotor speed to the pitch angle is obtained as follows:

$$\frac{\Theta(s)}{\Omega_m(s)} = \frac{K_{pp}D_t}{J_{pp}s^2 + D_{vp}s + K_{sp}}$$

By observing the denominator of the transfer function, it resembles the standard form of a second-order system:  $s^2 + 2\zeta\omega_n s + \omega_n^2$

Thus, by dividing the denominator by  $J_{pp}$ , the following can be concluded:

$$\begin{aligned}\frac{D_{vp}}{J_{pp}} &= 2\zeta\omega_n \\ D_{vp} &= 2J_{pp}\zeta\omega_n \\ \frac{K_{sp}}{J_{pp}} &= \omega_n^2 \\ K_{sp} &= J_{pp}\omega_n^2\end{aligned}$$

In task 11, it is asked to summarize the teamwork in the lab sessions. Overall, the teamwork was effective, and the division of workload among team members was well managed. Discussions between team members were conducted efficiently, contributing to a better understanding of the lab material and successful completion of lab tasks. Aspect that can be further improved is the speed of completing the lab task, as the work was finished very close to the deadline.

## Conclusions

The modelling and control design of the Quanser Aero2 Dual-Rotor system successfully met the objectives for controlling both the rotor and pitch subsystems in a 1 degree-of-freedom setup. For the rotor subsystem, step response analysis yielded a first-order model with a steady-state gain of 18.704 and a time constant of 1.16 seconds. Validation of this model revealed discrepancies, likely due to higher-order dynamics or nonlinear elements not accounted for in the model. For the pitch subsystem, step response and free oscillation observations were used to develop a second-order model, identifying key parameters such as the natural frequency,  $\omega_n = 0.735$  rad/s, and damping ratio,  $\zeta = 0.0167$ . Validation showed differences in phase shift and oscillation amplitude, due to underestimation of damping effects.

The first-order rotor subsystem was controlled by a PI with gain values used  $k_p = 0.027$  and  $k_i = 0.099$ . While the controller response performed well in simulation, the responses differed when applied to the physical Aero2 system. The second-order pitch subsystem was controlled by a PID controller with gain values used were  $k_p = 5.5$ ,  $k_i = 20$ , and  $k_d = 40$ , achieving good simulation performance but similarly showing discrepancies in physical implementation. These differences were likely due to unmodeled factors, such as friction and air resistance, which were not included in the models.

## Appendix

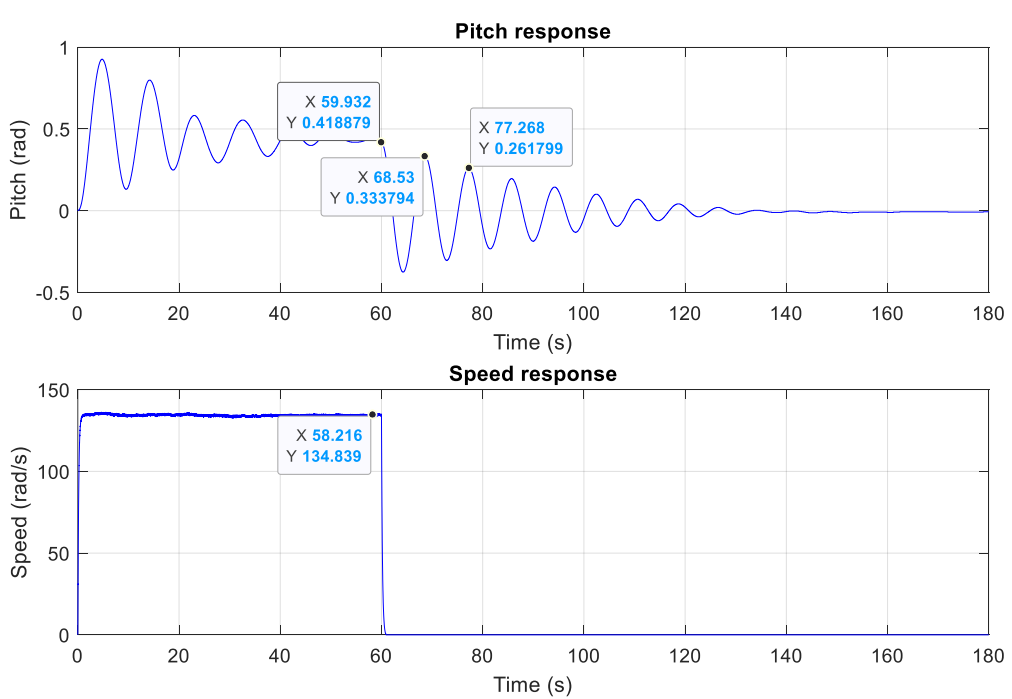
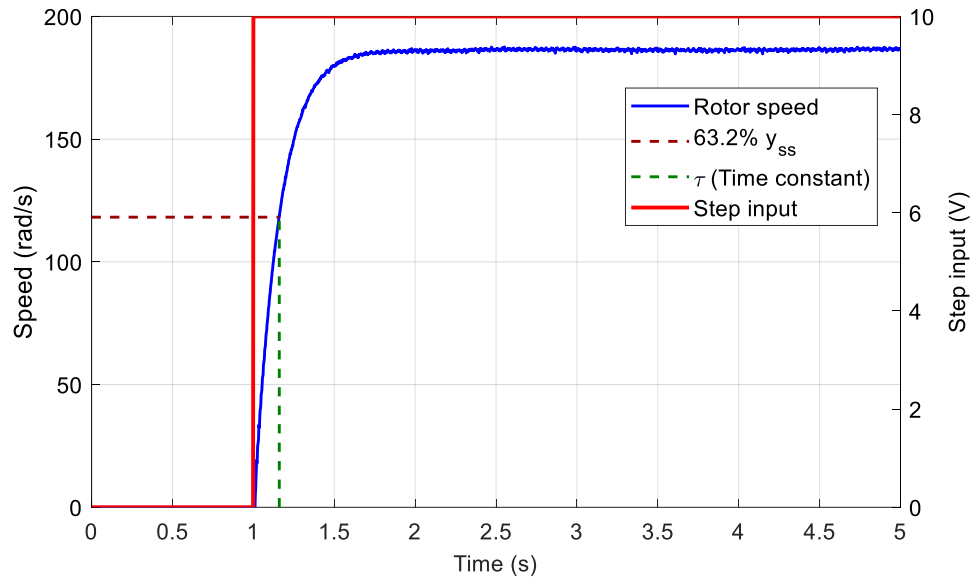


Figure B Model identification of pitch subsystem

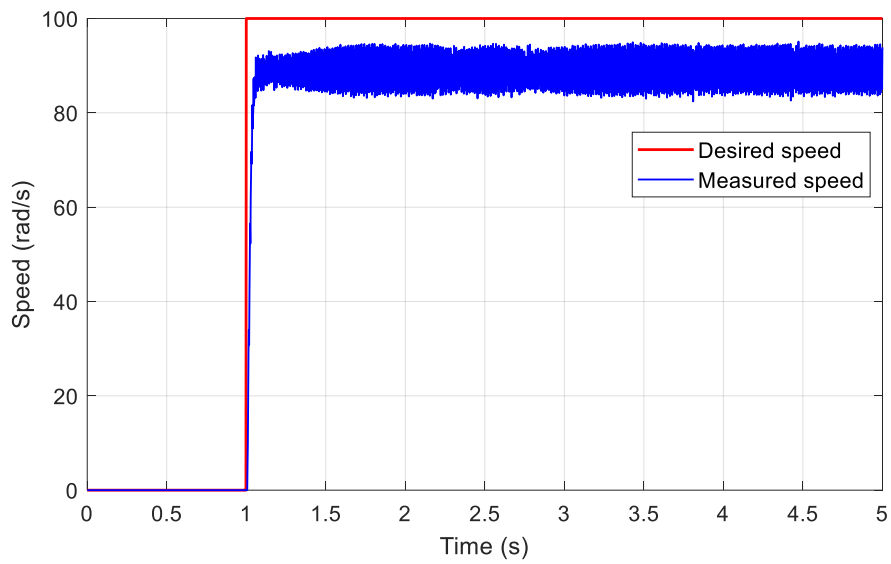


Figure C Step response of proportional controller familiarization

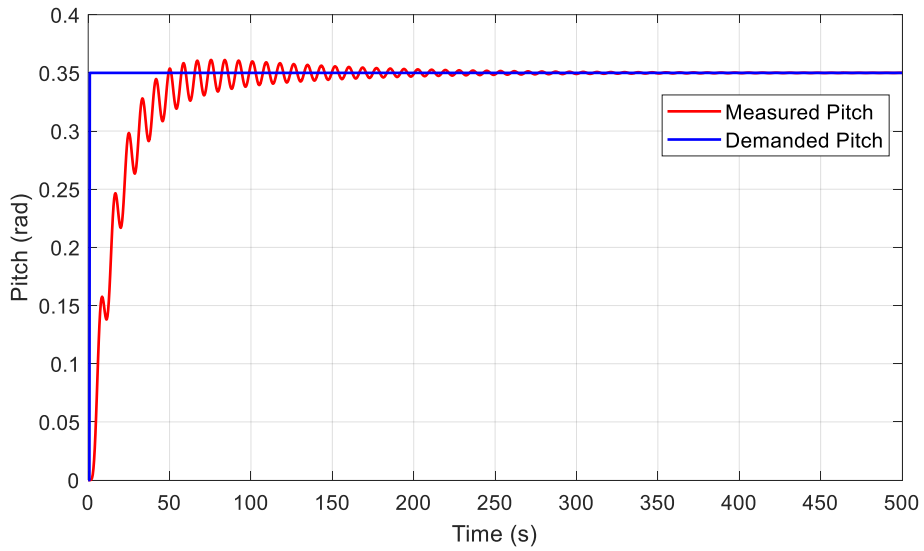


Figure D Simulated response of PID implementation controller on outer loop

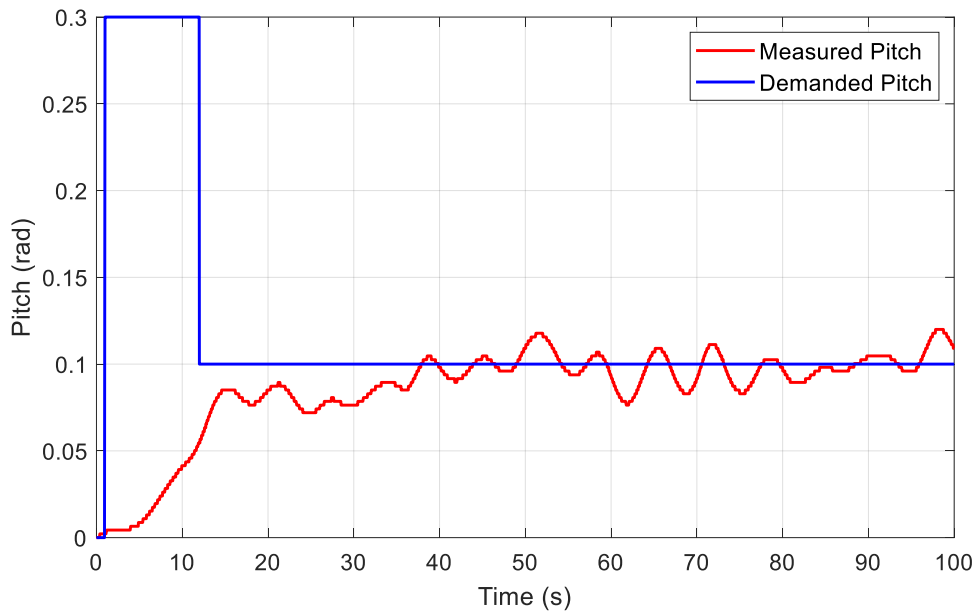


Figure E Measured response of PID controller implementation on outer loop